

In vitro oxidative degradation of a spinal posterior dynamic stabilisation device

Lawless, Bernard Michael; Espino, Daniel; Shepherd, Duncan

DOI:

[10.1002/jbm.b.33913](https://doi.org/10.1002/jbm.b.33913)

License:

Other (please specify with Rights Statement)

Document Version

Peer reviewed version

Citation for published version (Harvard):

Lawless, BM, Espino, D & Shepherd, D 2018, 'In vitro oxidative degradation of a spinal posterior dynamic stabilisation device', *Journal of Biomedical Materials Research. Part B: Applied Biomaterials*, vol. 106, no. 3, pp. 1237-1244. <https://doi.org/10.1002/jbm.b.33913>

[Link to publication on Research at Birmingham portal](#)

Publisher Rights Statement:

This is the peer reviewed version of the following article: Lawless BM, Espino DM, Shepherd DET. 2017. In vitro oxidative degradation of a spinal posterior dynamic stabilization device. *J Biomed Mater Res Part B* 2017, which has been published in final form at <http://dx.doi.org/10.1002/jbm.b.33913>. This article may be used for non-commercial purposes in accordance with Wiley Terms and Conditions for Self-Archiving.

General rights

Unless a licence is specified above, all rights (including copyright and moral rights) in this document are retained by the authors and/or the copyright holders. The express permission of the copyright holder must be obtained for any use of this material other than for purposes permitted by law.

- Users may freely distribute the URL that is used to identify this publication.
- Users may download and/or print one copy of the publication from the University of Birmingham research portal for the purpose of private study or non-commercial research.
- User may use extracts from the document in line with the concept of 'fair dealing' under the Copyright, Designs and Patents Act 1988 (?)
- Users may not further distribute the material nor use it for the purposes of commercial gain.

Where a licence is displayed above, please note the terms and conditions of the licence govern your use of this document.

When citing, please reference the published version.

Take down policy

While the University of Birmingham exercises care and attention in making items available there are rare occasions when an item has been uploaded in error or has been deemed to be commercially or otherwise sensitive.

If you believe that this is the case for this document, please contact UBIRA@lists.bham.ac.uk providing details and we will remove access to the work immediately and investigate.

1 Title Page

2 ***In vitro* oxidative degradation of a spinal posterior dynamic stabilisation**
3 **device**

4

5 **Bernard M. Lawless, Daniel M. Espino, Duncan E.T. Shepherd***

6 Department of Mechanical Engineering, School of Engineering, University of Birmingham,
7 United Kingdom

8

9 *Corresponding author: D.E.T Shepherd. Email: d.e.shepherd@bham.ac.uk

10 Tel: +441214144266 Fax: +4412141443958

11 **Abstract**

12 This study quantified the changes of the frequency-dependant viscoelastic properties of the
13 BDyn (S14 Implants, Pessac, France) spinal posterior dynamic stabilisation (PDS) device due
14 to *in vitro* oxidation. Six polycarbonate urethane (PCU) rings and six silicone cushions were
15 degraded by using a 20% hydrogen peroxide / 0.1M cobalt (II) chloride hexahydrate, at 37°C,
16 for 24 days. The viscoelastic properties of the individual components and the components
17 assembled into the BDyn PDS device were determined using Dynamic Mechanical Analysis
18 at frequencies from 0.01–30 Hz. Attenuated Total Reflectance Fourier Transform Infra-Red
19 spectra demonstrated chemical structure changes, of the PCU, associated with oxidation
20 while Scanning Electron Microscope images revealed surface pitting. No chemical structure
21 or surface morphology changes were observed for the silicone cushion. The BDyn device
22 storage and loss stiffness ranged between 84.46 N/mm to 99.36 N/mm and 8.13 N/mm to
23 21.99 N/mm, respectively. The storage and loss stiffness for the components and BDyn
24 device increased logarithmically with respect to frequency. Viscoelastic properties, between
25 normal and degraded components, were significantly different for specific frequencies only.
26 This study demonstrates the importance of analysing changes of viscoelastic properties of
27 degraded biomaterials and medical devices into which they are incorporated, using a
28 frequency sweep.

29 **Keywords:** BDyn Implant, Dynamic Mechanical Analysis, Oxidation, Posterior Dynamic
30 Stabilisation, Viscoelastic Properties.

31 Introduction

32 Spinal fusion is the gold standard for surgical treatment of low back pain caused by
33 degenerative disorders ^{(1)–(3)}. Many problems, such as adjacent segment degeneration and
34 pseudarthrosis, are associated with spinal fusion and to alleviate these problems non-fusion
35 techniques have been developed ⁽⁴⁾. The BDyn device (S14 Implants, Pessac, France) is a
36 posterior dynamic stabilisation device that provides an alternative to spinal fusion. This non-
37 fusion device comprises a mobile titanium alloy rod, a fixed titanium alloy rod, a
38 polycarbonate urethane (PCU) ring and a silicone cushion (figure 1). The BDyn device has
39 been used in the treatment of degenerative lumbar spondylolisthesis ⁽⁵⁾ and an *in vitro* study
40 has shown that the device can successfully limit the range of motion following a
41 laminectomy of L4-L5 segment ⁽⁶⁾.

42 Since the human lumbar spine has been reported to be resonant between 4–5 Hz in the
43 seated position ^{(7),(8)}, the frequency-dependent viscoelastic properties of the BDyn device,
44 and its elastomeric components, were quantified by Dynamic Mechanical Analysis (DMA) ⁽⁹⁾.
45 By applying an oscillating force to a multi-component structure and analysing the out-of-
46 phase displacement response, the storage (k') and loss (k'') stiffness were calculated to
47 characterise the viscoelastic properties ⁽¹⁰⁾. The storage stiffness represents the elastic
48 portion and it defines the ability of a structure to store energy, while the loss stiffness
49 describes the ability of the structure to dissipate energy through heat and internal motions
50 ⁽¹⁰⁾. Lawless et al. ⁽⁹⁾ found that the viscoelastic properties of the BDyn device and its
51 components were frequency dependent, for the frequency range 0.01-30 Hz, and no
52 resonant frequencies were recorded for the device or its components over this frequency
53 range.

54 The human body is an aggressive environment for biomaterials ⁽¹¹⁾, thus, it is important that
55 the materials of an implant can withstand the environment in the human body and not
56 become degraded to a point where the implant cannot perform its intended function ⁽¹²⁾.
57 Orthopaedic implants undergo numerous loads in a cyclical and potentially vibratory
58 manner. Also, implants endure *in vivo* hydrolytic, enzymatic and oxidative degradation at
59 body temperature. Oxidative degradation, the scission of the polymer chains through
60 oxygen ⁽¹³⁾, has been shown to be an influence in the biodegradation of polyether urethane
61 (PEU) and PCU ⁽¹⁴⁾. PCU has been stated to be more biostable ⁽¹⁵⁾ due to the removal of the
62 ether linkages in the soft segment ^{(14),(15)}.

63 Numerous studies have used an *in vitro* degradation method, that involves placing the
64 biomaterial into a 20% hydrogen peroxide (H₂O₂) and 0.1M cobalt chloride (CoCl₂) solution
65 at 37°C ⁽¹⁶⁾⁻⁽²²⁾, to replicate oxidation. The Haber-Weiss chemical reaction produces hydroxyl
66 radicals from this H₂O₂/CoCl₂ solution and it is an appropriate model of the *in vivo* chemical
67 reaction that produces oxygen radicals present at the polymer/cell interface ⁽²³⁾. This *in vitro*
68 method has been shown to reproduce chemical and physical degradation similar to *in vivo*
69 oxidative degradation of PEU and PCU ^{(14),(20)}. Further, this *in vitro* H₂O₂/CoCl₂ solution has
70 been commonly used to degrade polyether-urethane urea (PEUU), PEU, PCU and silicone
71 modified PEU and PCU ^{(16)-(18),(20),(21)}. Many of these studies focus on the degradation of films
72 ^{(16)-(18),(20),(21)} or standard tensile specimen shapes ⁽¹⁶⁾ to understand how the degradation
73 affects the mechanical behaviour of a material and not how degradation affects polymeric
74 components of implants.

75 The purpose of this study was to quantify the change in viscoelastic properties, using DMA,
76 of elastomeric components from a BDyn device that have been degraded by *in vitro*

77 oxidation. Furthermore, these components were assembled into BDyn devices and
78 comparisons were made between the degraded elastomeric components and the devices.
79 Comparisons were made between the viscoelastic properties of the normal components ⁽⁹⁾
80 and the degraded components.

81 **Materials and methods**

82 Six silicone and six PCU components (figure 2) were obtained from S14 Implants (Pessac,
83 France) and were used for a previous study ⁽⁹⁾. These components, which were sterilised
84 with ethylene oxide (EtO) (Steriservices, Bernay, France) for the previous study, were
85 degraded by using a 20% hydrogen peroxide (H₂O₂) and 0.1M cobalt (II) chloride
86 hexahydrate (CoCl₂.6H₂O) oxidative solution. The *in vitro* accelerated ageing of the
87 components was performed at 37°C in a Grant JBN18 water bath (Grant Instruments,
88 Royston, UK). To maintain a relatively constant concentration of radicals, the solution was
89 changed every 3 days and the degradation period lasted 24 days ^{(17),(20)}. After the
90 degradation period, the specimens were rinsed with water and were dried in a vacuum
91 chamber (Island Scientific Ltd., Ventnor, United Kingdom) for 48 hours at room
92 temperature.

93 The viscoelastic properties of the degraded components were measured using a Bose
94 ElectroForce 3200 testing machine running WinTest 4.1 DMA software (now, TA
95 Instruments, New Castle, DE, USA). The DMA technique, machine and software have been
96 used to quantify the storage and loss stiffness of a posterior dynamic stabilisation device, its
97 components ⁽⁹⁾ and various biological tissues ^{(24),(25)}.

98 Similar to the previous study ⁽⁹⁾, custom-designed grips were used to clamp the titanium
99 alloy rods and/or titanium alloy elastomer housing of the BDyn device. The devices were
100 secured by twelve horizontal screws. The order of component testing was randomised by
101 using the Excel Random Function (Redmond, Washington, USA). The degraded components
102 were then paired randomly and tested in the BDyn device. For testing of the BDyn 1 level,
103 the titanium alloy mobile and fixed rods were gripped. Since the BDyn device is designed to
104 work in both tension and compression, a sinusoidally varying load between +20 N (tension)
105 and -20 N (compression) was applied to the devices. As the components are only loaded in
106 compression, a sinusoidally varying load between -1 N and -20 N (compression) was applied
107 to the elastomeric components. Testing the device and components to these ranges gave a
108 direct comparison between the degraded components, the device and the previous study ⁽⁹⁾.
109 Initially, the degraded individual components were tested then the PCU and silicone
110 components were randomly paired, assembled in the BDyn titanium housing and tested. All
111 testing was performed, in air at 37°C ± 1°C, in a custom built chamber in which water was
112 pumped around the chamber while the air temperature was monitored throughout the
113 frequency sweep (figure 3).

114 The storage and loss stiffness were calculated for 21 different frequencies from 0.01 Hz to
115 30 Hz; this range is comparable to that of a previous study of the BDyn components ⁽⁹⁾. For
116 each frequency (f), a Fourier analysis of the force and displacement waves was performed
117 and the magnitude of the load (F^*), magnitude of the displacement (d^*), the phase lag (δ)
118 and the actual frequency were quantified ⁽⁹⁾. The complex stiffness (k^*), storage stiffness (k')
119 and loss stiffness (k'') were then calculated using ^{(9),(26),(27)}:

$$120 \quad k^* = \frac{F^*}{d^*} \quad (1)$$

121
$$k' = k^* \cos \delta \quad (2)$$

122
$$k'' = k^* \sin \delta \quad (3)$$

123 Attenuated Total Reflectance Fourier Transform Infra-Red (ATR-FTIR) spectroscopy was then
124 performed using a Bruker LUMOS spectrometer (Bruker Optics, Billerica, MA, USA). Spectra
125 were recorded in absorbance mode with a Germanium ATR crystal. Twenty spectra, with a
126 resolution of 2 cm^{-1} between 600 and 4000 cm^{-1} , were acquired and averaged to obtain each
127 spectrum ⁽²⁸⁾. The PCU spectra were normalised to the internal reference 1591 cm^{-1} peak,
128 the C=C bond stretch of the aromatic ring of the hard segment ^{(20),(29)-(31)}, which has been
129 shown to remain unchanged in degradation ⁽³²⁾.

130 The surface morphology of the elastomers was examined using the Hitachi TM3030
131 Scanning Electron Microscope (SEM) (Chiyoda, Tokyo, Japan). Specimens were sputter
132 coated with $\sim 30 \text{ nm}$ layer of gold by using an Agar B7340 sputter coater (Agar Scientific,
133 Stansted, Essex, UK). The specimens were examined with back-scatter detector at a 15 keV
134 accelerating voltage.

135 All statistical analyses were performed using SigmaPlot 13.0 (SYSTAT, San Jose, CA, USA).
136 95% confidence intervals were calculated ($n = 6$) and regression analyses were performed to
137 evaluate the significance of the curve fit. Wilcoxon signed rank tests were performed to
138 compare the differences of the components before and after degradation. Whereas a
139 Wilcoxon rank sum test compared the normal BDyn viscoelastic properties ⁽⁹⁾ to the BDyn
140 device assembled with the degraded components. Statistical results with $p < 0.05$ were
141 considered significant.

142 **Results**

143 The ATR-FTIR spectrum, of the PCU and silicone components, is illustrated in figure 4 and
144 figure 5, respectively. Evidence of crosslinking of the PCU has been established as a new
145 absorbance peak was observed at 1174 cm^{-1} . The PCU degraded specimens also showed
146 hard segment degradation with the presence of a new aromatic amine group at 1650 cm^{-1} .
147 There was no evidence of changes to the chemical structure of the degraded silicone
148 specimens (figure 5).

149 Representative SEM images of the surfaces of the PCU and silicone components are shown
150 in figure 6 and figure 7, respectively. The PCU specimens degraded for 24 days
151 demonstrated surface pitting. There was no evidence of surface pitting, or any other
152 surface morphology changes, with the degraded silicone specimens.

153 Figure 8 presents the storage stiffness of the (a) BDyn implant, (b) PCU component and (c)
154 silicone component, for normal and degraded components. The mean degraded PCU and
155 silicone components storage stiffness ranged between 87.5 N/mm to 135.3 N/mm and 51.6
156 N/mm to 60.7 N/mm , respectively. The BDyn implant storage stiffness ranged between
157 84.46 N/mm to 99.36 N/mm . The storage stiffness logarithmically increased in relation to
158 frequency ($p < 0.05$) (equation 4, where A is a coefficient and B is a constant, and Table 1).

159
$$k' = A \ln(f) + B \quad \text{for } 0.01 \leq f \leq 30 \quad (4)$$

160 Figure 9 exhibits the normal and degraded loss stiffness for the (a) BDyn implant, (b) PCU
161 component and (c) silicone component. The degraded PCU and silicone components loss
162 stiffness ranged between 6.03 N/mm to 24.45 N/mm and 4.59 N/mm to 10.83 N/mm ,
163 respectively. The BDyn implant loss stiffness ranged between 8.13 N/mm to 21.99 N/mm .

164 Similarly to the storage stiffness, the loss stiffness logarithmically increased in relation to
165 frequency ($p < 0.05$) (equation 5, where C is a coefficient and D is a constant, and Table 1).

$$166 \quad k'' = C \ln(f) + D \quad \text{for } 0.01 \leq f \leq 30 \quad (5)$$

167 For the PCU component, silicone component and BDyn implant assembled with the
168 degraded components, the storage stiffness was larger than the loss stiffness for all
169 frequencies tested. Table 2 provides the frequencies at which the PCU and silicone
170 components were significantly different before and after degradation. The storage and loss
171 stiffness of the silicone component, before and after degradation, were significantly
172 different for the frequency range tested while the PCU component loss stiffness was only
173 significantly different for certain frequencies; 0.5 Hz, 4 Hz to 30 Hz. Also, the storage
174 stiffness of the BDyn device, assembled with degraded components, was significantly
175 different from 0.2 Hz to 20 Hz while, the loss stiffness was significantly different from 0.01
176 Hz to 0.3 Hz and 0.5 Hz to 15 Hz.

177 **Discussion**

178 This study has quantified the frequency-dependent viscoelastic properties of a posterior
179 dynamic stabilisation device with *in vitro* oxidative degraded components. The degraded
180 components and BDyn device, with the degraded components, were viscoelastic throughout
181 the frequency range tested. The degraded BDyn 1 level device storage stiffness and loss
182 stiffness were less than the storage stiffness (95.56 N/mm to 119.29 N/mm) and loss
183 stiffness (10.72 N/mm to 23.42 N/mm) ⁽⁹⁾ for the normal BDyn 1 level device. However, the
184 reductions in viscoelastic properties of the PCU and silicone components, due to the *in vitro*
185 degradation process, are significantly different for specific frequencies. Subsequently, the

186 storage and loss stiffness of the BDyn device assembled with *in vitro* degraded components
187 were lower than those of the untreated device ⁽⁹⁾ only for specific frequencies. These
188 findings demonstrate the importance of analysing changes of viscoelastic properties of
189 specimens over a frequency sweep.

190 The mean storage stiffness and mean loss stiffness trends of the BDyn device and
191 components followed a logarithmic increasing trend with frequency; these trends are
192 similar to the normal, untreated specimens ⁽⁹⁾. This is deemed a positive result as the
193 degradation did not affect the frequency-dependant behaviour of the components or
194 device. However, the logarithmic equation coefficients (*A* and *C*) and constants (*B* and *D*) of
195 the degraded specimens were lower than the normal specimens ⁽⁹⁾. Similarly to the normal
196 BDyn implant and components ⁽⁹⁾, no resonant frequencies were identified for the degraded
197 components and implant with degraded components. Previous studies ^{(33),(34)} have also
198 shown that the lumbar specimens did not exhibit shock absorbing properties, in pure
199 compression, as no sharp peak detected in the loss modulus for the frequency range ⁽³³⁾.
200 Panjabi et al. ⁽⁷⁾ recorded the average *in vivo* lumbar vertebrae resonant frequency at 4.4 Hz
201 for the axial direction, in the seated position. Wilder et al. ⁽⁸⁾ recorded the greatest
202 transmissibility in the male and female lumbar spine of 4.9 Hz and 4.75 Hz, respectively, and
203 also recorded two further resonant frequencies at 9.5 Hz and 12.7 Hz. Any resonance, of the
204 device, at any frequency is a limitation of the device as the resonance may damage the
205 device and in a worst case scenario, the device may fail ⁽⁹⁾.

206 Other studies have examined the effect of *in vitro* oxidative degradation in relation to
207 tensile strain ^{(16),(22),(31)} and Dynamic Mechanical Thermal Analysis (DMTA) ^{(17),(35)}, but not
208 DMA. After 36 days of *in vitro* oxidation, Dempsey et al. ⁽¹⁶⁾ stated that the ultimate tensile

209 strength of Bionate 80A, a PCU, was less when compared to the untreated specimens.
210 However, the ultimate tensile strength of Bionate II 80A was greater for the specimens that
211 were treated; the percentage elongation of Bionate 80A and Bionate II 80A increased by 2-
212 3% after oxidation ⁽¹⁶⁾. Schubert et al. ⁽²¹⁾ discovered a 10% decrease in stress at high strains
213 of treated PEUU specimens when compared to the untreated PEUU specimens. This result
214 was similar to those of Christenson et al. ⁽²⁰⁾ who found a minor decrease in stress at high
215 strains when comparing the tensile stress-strain behaviour of *in vitro* oxidised PEU and PCU
216 to untreated PEU and PCU. Apart from this decrease in stress, the Young's modulus was
217 unaffected ⁽²⁰⁾. By using DMTA, Wu et al. ⁽³⁵⁾ investigated the biostability of polyether
218 urethane urea (PEUU) blood sacs and proposed a greater degree of phase separation
219 between hard and soft segments of the implanted sacs due to the α transition shift of -15°C,
220 compared to the control. Hernandez et al. ⁽¹⁷⁾ discovered that the maximum loss factor (tan
221 δ), of a PCU, reduced by approximately 0.05 while the storage modulus did not appreciably
222 change after oxidation. From this, the author suggested that there was no significant
223 changes in the hard-soft segment organisation in the bulk ⁽¹⁷⁾. This lack of appreciable
224 change is similar to the present study as the storage stiffness, of the PCU, was not
225 significantly different following degradation over the frequency range tested. However, in
226 the present study, the viscous property (loss stiffness), of the PCU component, was affected
227 by *in vitro* oxidation at 0.5 Hz and from 4 Hz to 30 Hz. This demonstrates the importance of
228 understanding the viscoelastic properties of components and implants in relation to
229 frequency.

230 Christenson et al. ⁽²⁰⁾ demonstrated that *in vitro* degradation of PEU and PCU, with the 20%
231 hydrogen peroxide (H₂O₂) and 0.1M cobalt chloride (CoCl₂) solution at 37 °C for 24 days, led

232 to surface pitting and ATR-FTIR spectra changes. Such changes were similar to explanted
233 PCU rods from rabbits after 15 months and PCU specimens from rats after 20 weeks⁽³¹⁾.
234 From the ATR-FTIR spectrum, a decrease in absorbance peak intensity at 1247 cm⁻¹ was
235 observed for the degraded PCU; this decrease, along with the new absorbance peak at 1174
236 cm⁻¹ provides evidence of chain scission and crosslinking of the soft segment^{(17),(20),(36)}. A
237 decrease of the degraded PCU hard segment urethane intensity and a new absorbance peak
238 at 1650 cm⁻¹ (the potential degradation product of the aromatic amine⁽³¹⁾) provides
239 evidence of hard segment chain scission^{(20),(23),(30)}. These spectrum changes are similar to
240 previous work^{(20),(30)} however, the new peaks observed at 1174 cm⁻¹ and 1650 cm⁻¹ are not
241 as prominent as previous studies^{(20),(18)} and this may be due to the antioxidant inhibitor
242 used in this commercially available PCU. This inhibitor will have had an effect on the
243 degradation and, in turn, the absorbance peaks at 1174 cm⁻¹ and 1650 cm⁻¹. However, the
244 degraded PCU ATR-FTIR spectrum absorbance peaks at 1174 cm⁻¹ and 1650 cm⁻¹, from our
245 current study, are similar to another study⁽¹⁶⁾ that degraded PCU specimens with an
246 accelerated oxidation method for 36 days. In the present study, SEM images revealed pitting
247 on the surface of the PCU components which has been previously documented for *in vitro*
248 and *in vivo* oxidation of PCU^{(16),(31)}.

249 Explanted orthopaedic implants, which contain PCU components, have demonstrated new
250 absorbance peaks at 1650 cm⁻¹ and/or 1174 cm⁻¹ to demonstrate biological oxidative
251 degradation⁽³⁷⁾⁻⁽³⁹⁾. However, another explant study did not find new absorbance peaks
252 linked to biological oxidative degradation⁽⁴⁰⁾. Ianuzzi et al.⁽³⁹⁾ stated that the majority of the
253 PCU spacers, exhibiting a chemical change associated with biodegradation, experienced this
254 degradation on the surface where the spacer would make contact with tissue. Examination

255 of retrieved PCU spacers revealed that chemical changes were negligible 100 μm below the
256 surface ⁽⁴¹⁾. The elastomeric components of the BDyn device are surrounded by titanium
257 alloy housing (see figure 2). In this study, the components were completely exposed to the
258 $\text{H}_2\text{O}_2/\text{CoCl}_2$ solution without taking into account the effect of the titanium alloy housing. It is
259 hypothesised that the titanium housing will have an effect on the degradation of the
260 polymer components. The titanium alloy housing may protect the components from
261 biodegradation, or alternatively, additional titanium alloy may increase metal ion oxidation
262 (MIO).

263 Silicone has demonstrated excellent biostability with no identifiable *in vivo* degradation ⁽⁴²⁾
264 and due to this excellent biostability, silicone has been used to modify PEU and PCU to
265 increase the biostability with the intention to inhibit degradation. The oxidation method,
266 used in this study, has been previously used to understand how degradation affects
267 PCU/PEU ^{(16)–(18),(20),(21)} and PCU/PEU modified with silicone ⁽¹⁸⁾. In comparison to unmodified
268 PEU and PCU, the percent loss of silicone-modified PEU and PCU soft-segment was less than
269 the unmodified PEU and PCU; this may be an indication of slower rates of crosslinking due
270 to the addition on silicone ⁽¹⁸⁾. The $\text{H}_2\text{O}_2/\text{CoCl}_2$ *in vitro* method has been shown to reproduce
271 chemical and physical degradation similar to *in vivo* oxidative degradation of PEU and PCU
272 ^{(14),(20)}, but not for silicone. It was expected that there would be no significant change in the
273 viscoelastic properties of the silicone cushion, by using this $\text{H}_2\text{O}_2/\text{CoCl}_2$ degradation method.
274 However, the storage and loss stiffness of the treated silicone component was significantly
275 different, for every frequency tested, when compared to viscoelastic properties before
276 degradation. That said, there were no changes evident in the ATR-FTIR spectra and unlike

277 the PCU ring, no pitting or surface morphology changes were observed for the silicone
278 cushions.

279 As the dynamic stiffness can be affected by load ⁽⁴³⁾, any comparison between different
280 methods and studies must be made with caution ⁽⁹⁾. For consistency to our previous study,
281 the methods all remained unchanged with the only change being the degradation of the
282 PCU and silicone components; this was important to understand how the *in vitro*
283 degradation process affects the frequency dependent viscoelastic properties. Regardless, no
284 *in vitro* degradation method fully replicates the biochemical and biomechanical stresses
285 experienced in the body ⁽⁴²⁾. Consistent with our previous study, the DMA test configuration
286 is not similar to the *in vivo* scenario where the mobile and fixed rods are secured to the
287 pedicles⁽⁹⁾. By securing the mobile rod to the vertebra, an applied load to the device may not
288 displace the two polymer systems equally; hence, the difference in displacement will affect
289 the dynamic stiffness (k^*) and in turn, the storage (k') and loss (k'') stiffness ⁽⁹⁾. The BDyn
290 device is designed to allow partial movement along the anatomical planes⁽⁹⁾. This study
291 quantified the viscoelastic properties of the degraded BDyn components, and the degraded
292 components in the device, uniaxially. Rotation of the moveable rod, around an anatomical
293 plane, may affect the response of the out-of-phase displacement to an applied force and
294 hence, affect the viscoelastic properties ⁽⁹⁾. However, these limitations do not alter the
295 conclusions of this study because the sinusoidally applied loads ensured a direct comparison
296 between the normal and degraded components and implant.

297 In conclusion, two viscoelastic components of a spinal posterior dynamic stabilisation device
298 were treated by an *in vitro* oxidation method. Only the PCU components displayed changes
299 to their chemical structure and exhibited surface morphology changes. The loss stiffness,

300 between normal and degraded components, of the PCU component were significantly
301 different for specific frequencies while the storage and loss stiffness of the silicone
302 component were significantly different for all frequencies tested. When compared to the
303 untreated BDyn device, the storage and loss stiffness of the BDyn device assembled with the
304 *in vitro* degraded components were statistically different for certain frequencies. This study
305 demonstrates the importance of analysing changes of viscoelastic properties, of degraded
306 biomaterials, in terms of frequency and medical devices into which they are incorporated,
307 using a frequency sweep.

308 **Acknowledgments**

309 The authors would like to thank Carl Hingley, Peter Thornton, Lee Gauntlett, Jack Garrod,
310 Becky Charles and Adam Sheward from the Department of Mechanical Engineering, School
311 of Engineering and Daniel P. Smith from the Birmingham Centre for Cryogenic Energy
312 Storage, School of Chemical Engineering, University of Birmingham for their assistance with
313 experimental testing. Also, the authors would like to thank Terence Green from the School
314 of Chemistry, University of Birmingham and Ronan Dorrepaal from University College Dublin
315 for discussions in chemistry matters. This study was supported by the European Commission
316 under the 7th Framework Programme (Grant agreement no.: 604935). The DMA equipment
317 used in this study was funded by Arthritis Research UK (Grant Number: H0671).

318 **Conflict of Interest**

319 The University of Birmingham and S14 Implants are beneficiaries of the support by the
320 European Commission under the 7th Framework Programme (Grant agreement no.:

321 604935). No employees of S14 Implants were involved in this study and no benefit of any
322 kind will be received either directly or indirectly by the author(s).

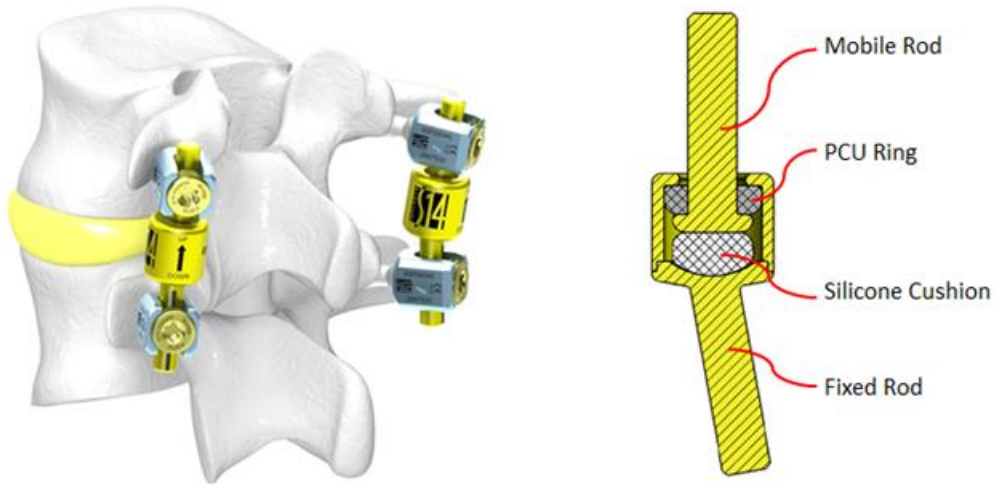
323 **References**

- 324 1. Schwarzenbach O, Rohrbach N, Berlemann U. Segment-by-segment stabilization for
325 degenerative disc disease: A hybrid technique. *Eur Spine J.* 2010;19:1010–20.
- 326 2. Sengupta DK. Dynamic stabilization devices in the treatment of low back pain. *Orthop*
327 *Clin North Am.* 2004;35:43–56.
- 328 3. van den Broek PR, Huyghe JM, Wilson W, Ito K. Design of next generation total disk
329 replacements. *J Biomech.* 2012;45:134–40.
- 330 4. Serhan H, Mhatre D, Defossez H, Bono CM. Motion-preserving technologies for
331 degenerative lumbar spine: The past, present and future horizons. *SAS J.* 2011;5:75–
332 89.
- 333 5. Gille O, Challier V, Parent H, Cavagna R, Poignard A, Faline A, Fuentes S, Ricart O,
334 Ferrero E, Ould Slimane M. Degenerative lumbar spondylolisthesis. Cohort of 670
335 patients, and proposal of a new classification. *Orthop Traumatol Surg Res.*
336 2014;100:311–5.
- 337 6. Guerin P, Gille O, Persohn S, Campana S, Vital JM, Skalli W. Effect of new dynamic
338 stabilization system on the segmental motion and intradiscal pressure: An in vitro
339 biomechanical study. *ORS 2011 Annu Meet.* 2011.
- 340 7. Panjabi MM, Andersson GB, Jorneus L, Hult E, Mattsson L. In vivo measurements of
341 spinal column vibrations. *J Bone Jt Surg.* 1986;68:695–702.
- 342 8. Wilder DG, Woodworth BB, Frymoyer JW, Pope MH. *Vibration and the human spine.*
343 *Spine (Phila Pa 1976).* 1982;7:243–54.
- 344 9. Lawless BM, Barnes SC, Espino DM, Shepherd DET. Viscoelastic properties of a spinal
345 posterior dynamic stabilisation device. *J Mech Behav Biomed Mater.* 2016;59:519–26.
- 346 10. Menard KP. *Dynamic Mechanical Analysis: A Practical Introduction.* 2nd ed. Boca
347 Raton, Florida: CRC press, Taylor & Francis Group; 2008.
- 348 11. Ramakrishna S, Mayer J, Wintermantel E, Leong KW. Biomedical applications of
349 polymer-composite materials: a review. *Compos Sci Technol.* 2001;61:1189–224.
- 350 12. Gurappa I. Characterization of different materials for corrosion resistance under
351 simulated body fluid conditions. *Mater Charact.* 2002;49:73–9.
- 352 13. ISO. *BS EN ISO 10993-13: Identification and quantification of degradation products*
353 *from polymeric medical device.* 2010.
- 354 14. Chandy T, Van Hee J, Nettekoven W, Johnson J. Long-term in vitro stability
355 assessment of polycarbonate urethane micro catheters: resistance to oxidation and
356 stress cracking. *J Biomed Mater Res Part B Appl Biomater.* 2009;89:314–24.

- 357 15. Tanzi MC, Mantovani D, Petrini P, Guidoin R, G L. Chemical stability of polyether
358 urethanes versus polycarbonate urethanes. *J Biomed Mater Res.* 1997;36:550–9.
- 359 16. Dempsey DK, Carranza C, Chawla CP, Gray P, Eoh JH, Cereceres S, Cosgriff-hernandez
360 EM. Comparative analysis of in vitro oxidative degradation of poly (carbonate
361 urethanes) for biostability screening. *J Biomed Mater Res Part A.* 2014;102:3649–65.
- 362 17. Hernandez R, Weksler J, Padsalgikar A, Runt J. In vitro oxidation of high
363 polydimethylsiloxane content biomedical polyurethanes: correlation with the
364 microstructure. *J Biomed Mater Res Part A.* 2008;87:546–56.
- 365 18. Christenson EM, Dadsetan M, Anderson JM, Hiltner A. Biostability and macrophage-
366 mediated foreign body reaction of silicone-modified polyurethanes. *J Biomed Mater
367 Res Part A.* 2005;74:141–55.
- 368 19. Sarkar D, Lopina ST. Oxidative and enzymatic degradations of L-tyrosine based
369 polyurethanes. *Polym Degrad Stab.* 2007;92:1994–2004.
- 370 20. Christenson EM, Anderson JM, Hiltner A. Oxidative mechanisms of poly(carbonate
371 urethane) and poly(ether urethane) biodegradation: In vivo and in vitro correlations. *J
372 Biomed Mater Res Part A.* 2004;70:245–55.
- 373 21. Schubert MA, Wiggins MJ, Anderson JM, Hiltner A. Role of oxygen in biodegradation
374 of poly(etherurethane urea) elastomers. *J Biomed Mater Res.* 1997;34:519–30.
- 375 22. Andriani Y, Morrow IC, Taran E, Edwards GA, Schiller TL, Osman AF, Martin DJ. In vitro
376 biostability of poly(dimethyl siloxane/hexamethylene oxide)-based
377 polyurethane/layered silicate nanocomposites. *Acta Biomater.* 2013;9:8308–17.
- 378 23. Christenson EM, Anderson JM, Hiltner A. Biodegradation mechanisms of
379 polyurethane elastomers. *Corros Eng Sci Technol.* 2007;42:312–23.
- 380 24. Barnes SC, Lawless BM, Shepherd DET, Espino DM, Bicknell GR, Bryan RT. Viscoelastic
381 Properties of Human Bladder Tumours. *J Mech Behav Biomed Mater.* 2016;61:250–7.
- 382 25. Omari EA, Varghese T, Kliewer MA, Harter J, Hartenbach EM. Dynamic and quasi-
383 static mechanical testing for characterization of the viscoelastic properties of human
384 uterine tissue. *J Biomech.* 2015;48:1730–6.
- 385 26. Fulcher GR, Hukins DWL, Shepherd DET. Viscoelastic properties of bovine articular
386 cartilage attached to subchondral bone at high frequencies. *BMC Musculoskelet
387 Disord.* 2009;10;61.
- 388 27. Barnes SC, Shepherd DET, Espino DM, Bryan RT. Frequency dependent viscoelastic
389 properties of porcine bladder. *J Mech Behav Biomed Mater.* 2015;42:168–76.
- 390 28. Simmons A, Hyvarinen J, Odell RA, Martin DJ, Gunatillake PA, Noble KR, Poole-Warren
391 LA. Long-term in vivo biostability of poly(dimethylsiloxane)/poly(hexamethylene
392 oxide) mixed macrodiol-based polyurethane elastomers. *Biomaterials.* 2004;25:4887–
393 900.
- 394 29. Padsalgikar A, Cosgriff-Hernandez E, Gallagher G, Touchet T, Iacob C, Mellin L, Norlin-
395 weissenrieder A, Runt J. Limitations of predicting in vivo biostability of multiphase
396 polyurethane elastomers using temperature-accelerated degradation testing. *J*

- 397 Biomed Mater Res Part B Appl Biomater. 2015;103:159–68.
- 398 30. Christenson EM, Anderson JM, Hiltner A. Antioxidant inhibition of poly(carbonate
399 urethane) in vivo biodegradation. J Biomed Mater Res Part A. 2006;76:480–90.
- 400 31. Christenson EM, Dadsetan M, Wiggins M, Anderson JM, Hiltner A. Poly(carbonate
401 urethane) and poly(ether urethane) biodegradation: In vivo studies. J Biomed Mater
402 Res Part A. 2004;69A:407–16.
- 403 32. Wu Y, Sellitti C, Anderson JM, Hiltner A, Lodoen GA, Payet CR. An FTIR-ATR
404 Investigation of In Vivo Poly(ether urethane) Degradation. J Appl Polym Sci.
405 1992;46:201–11.
- 406 33. Holmes AD, Hukins DWL. Analysis of load-relaxation in compressed segments of
407 lumbar spine. J Med Eng Phys. 1996;18:99–104.
- 408 34. Gadd MJ, Shepherd DET. Viscoelastic properties of the intervertebral disc and the
409 effect of nucleus pulposus removal. Proc Inst Mech Eng Part H J Eng Med.
410 2011;255:335–41.
- 411 35. Wu L, Weisberg DM, Runt J, Felder G, Snyder AJ, Rosenberg G. An investigation of the
412 in vivo stability of poly(ether urethaneurea) blood sacs. J Biomed Mater Res.
413 1999;44:371–80.
- 414 36. Tanzi MC, Farè S, Petrini P. In vitro stability of polyether and polycarbonate
415 urethanes. J Biomater Appl. 2000;14:325–48.
- 416 37. Cipriani E, Bracco P, Kurtz SM, Costa L, Zanetti M. In-vivo degradation of
417 poly(carbonate-urethane) based spine implants. Polym Degrad Stab. 2013;98:1225–
418 35.
- 419 38. Neukamp M, Roeder C, Veruva SY, MacDonald DW, Kurtz SM, Steinbeck MJ. In vivo
420 compatibility of Dynesys spinal implants: a case series of five retrieved periprosthetic
421 tissue samples and corresponding implants. Eur Spine J. 2015;24:1074–84.
- 422 39. Ianuzzi A, Kurtz SM, Kane W, Shah P, Siskey R, Ooij A Van, Bindal R, Ross R, Lanman T,
423 Buttner-Janž K, Isaza J. In Vivo Deformation, Surface Damage, and Biostability of
424 Retrieved Dynesys Systems. Spine (Phila Pa 1976). 2010;35:1310–6.
- 425 40. Shen M, Zhang K, Koettig P, Welch WC, Dawson JM. In vivo biostability of polymeric
426 spine implants: retrieval analyses from a United States investigational device
427 exemption study. Eur Spine J. 2011;20:1837–49.
- 428 41. Trommsdorff U, Zurbrugg D, Abt N. Analysis of retrieved components of a dynamic
429 stabilization system for the spine. 68th Annu Meet Ger Soc Surg. Berlin, Germany;
430 2004.
- 431 42. Wilkoff BL, Rickard J, Tkatchouk E, Padsalgikar AD, Gallagher G, Runt J. The biostability
432 of cardiac lead insulation materials as assessed from long-term human implants. J
433 Biomed Mater Res Part B Appl Biomater. 2015;104:411–21.
- 434 43. Kasra M, Shirazi-Adl A, Drouin G. Dynamics of Human Lumbar Intervertebral Joints:
435 Experimental and Finite-Element Investigations. Spine (Phila Pa 1976). 1992;17:93–
436 102.

438 **Figure Legends**

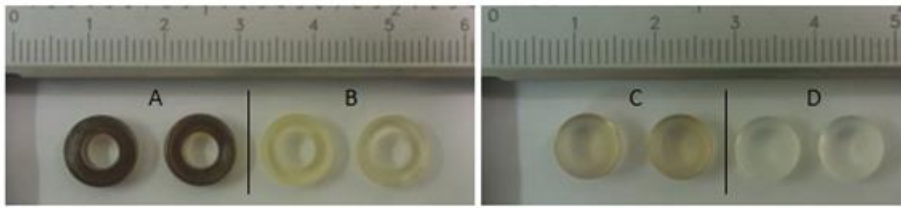


439

440 Figure 1: BDyn 1 level device fixed to the vertebrae (Left) [Reproduced with kind permission
441 from S14 Implants, Pessac, France. © S14 Implants] and cross sectional view of the BDyn
442 device (Right). The polycarbonate urethane (PCU) ring and silicone cushion components,
443 along with the mobile and fixed rods, are highlighted.

444

445



446

447 Figure 2: PCU components, (A) before and (B) after degradation, and silicone components
448 (C) before and (D) after degradation. The normal PCU and silicone components are used in
449 the BDyn device.

450

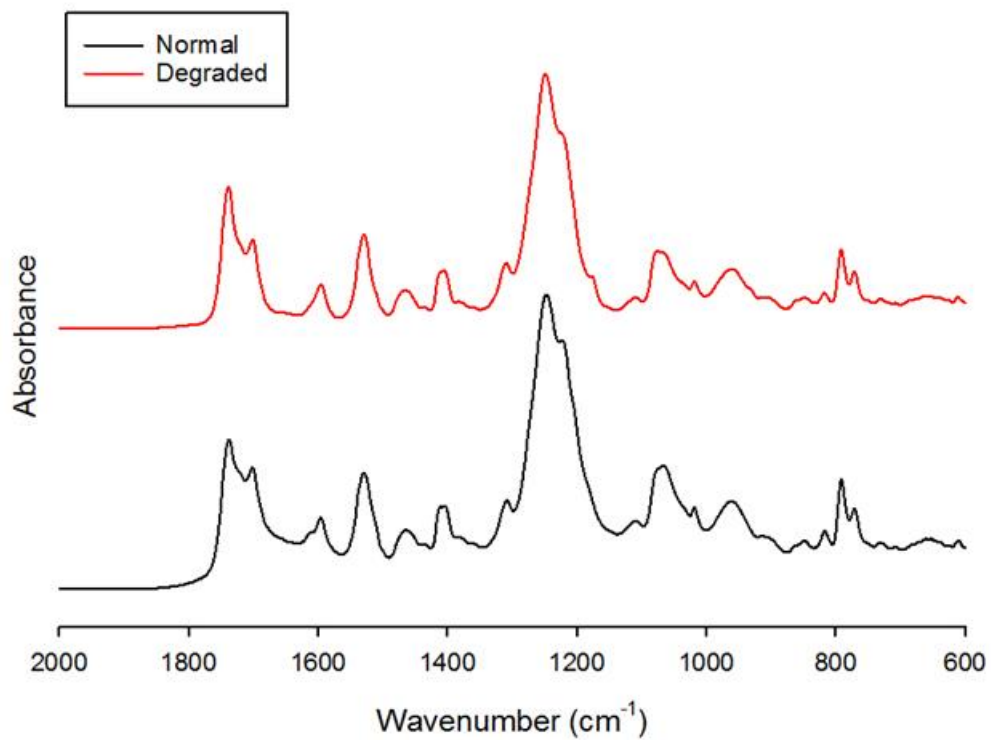
451



452

453 Figure 3: Testing of BDyn 1 device with degraded elastomer components in the custom built
454 chamber

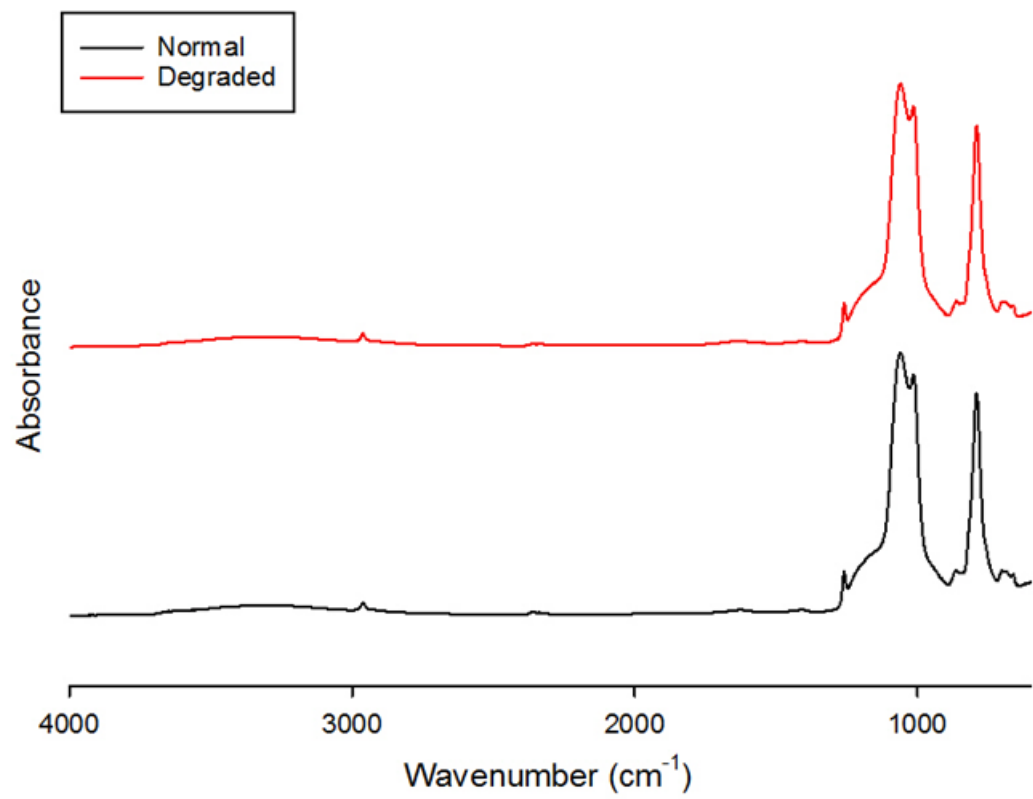
455



456

457 Figure 4: Stacked ATR-FTIR spectra of PCU components before (Normal) and after
458 (Degraded) *in vitro* oxidative degradation

459

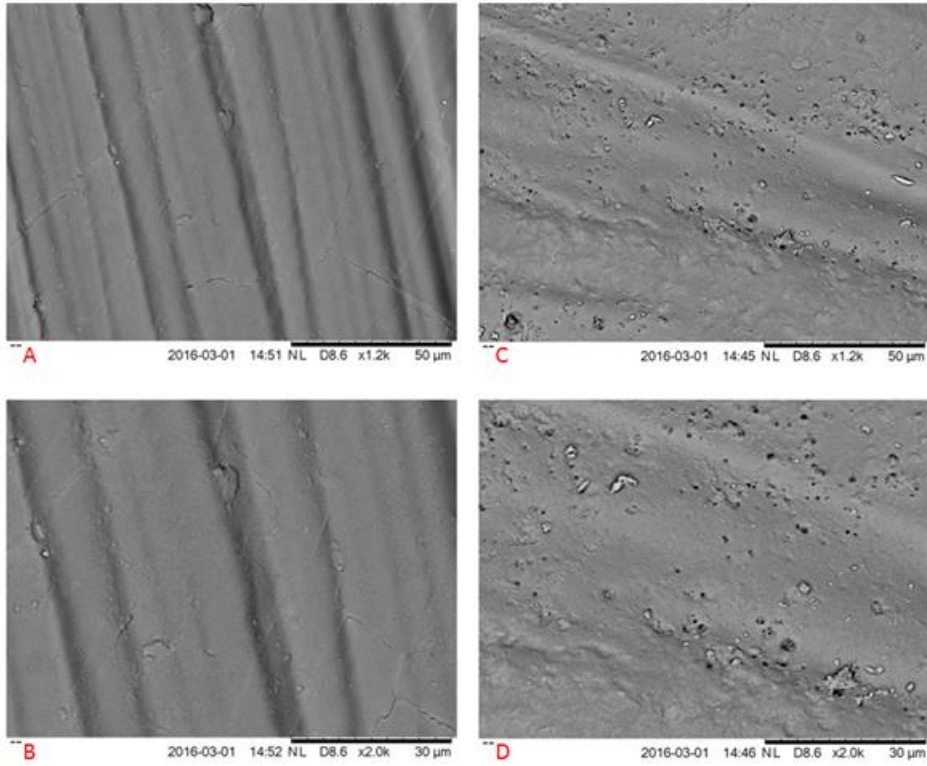


460

461 Figure 5: Stacked ATR-FTIR spectra of silicone components before (Normal) and after

462 (Degraded) *in vitro* oxidative degradation

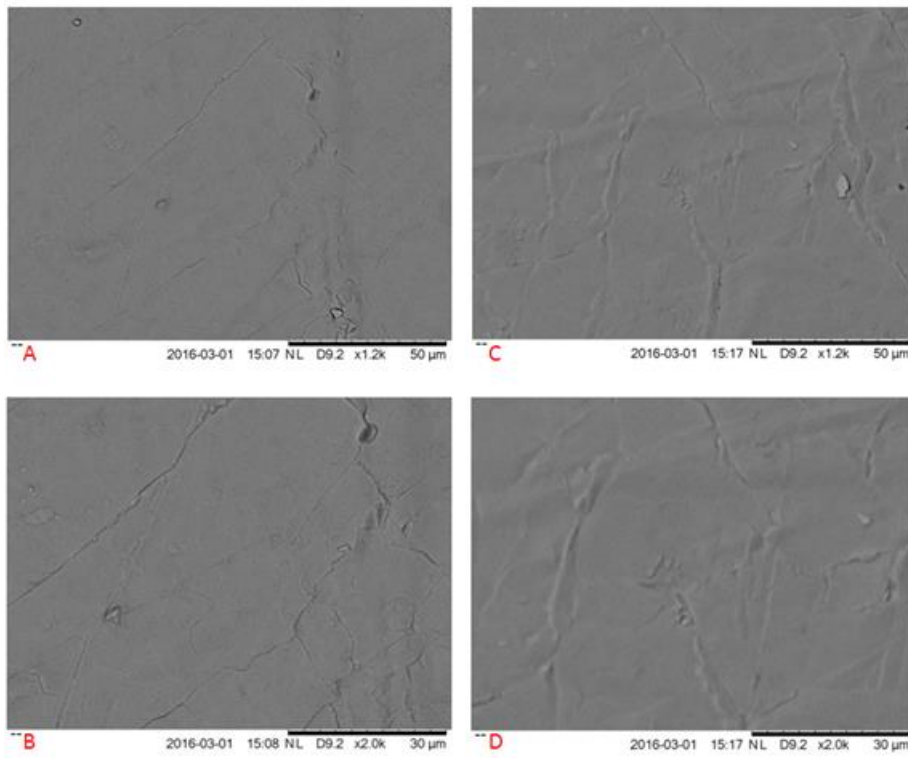
463



464

465 Figure 6: Scanning electron micrographs of PCU components before, at (A) ×1.2k and (B)
466 ×2.0k magnification, and after, at (C) ×1.2k and (D) ×2.0k magnification, *in vitro* oxidative
467 degradation

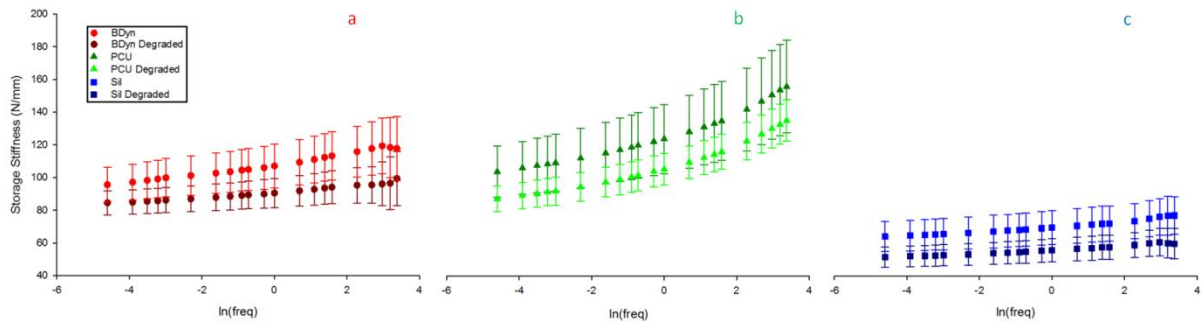
468



470

471 Figure 7: Scanning electron micrographs of silicone components before, at (A) $\times 1.2k$ and (B)
472 $\times 2.0k$ magnification, and after, at (C) $\times 1.2k$ and (D) $\times 2.0k$ magnification, *in vitro* oxidative
473 degradation

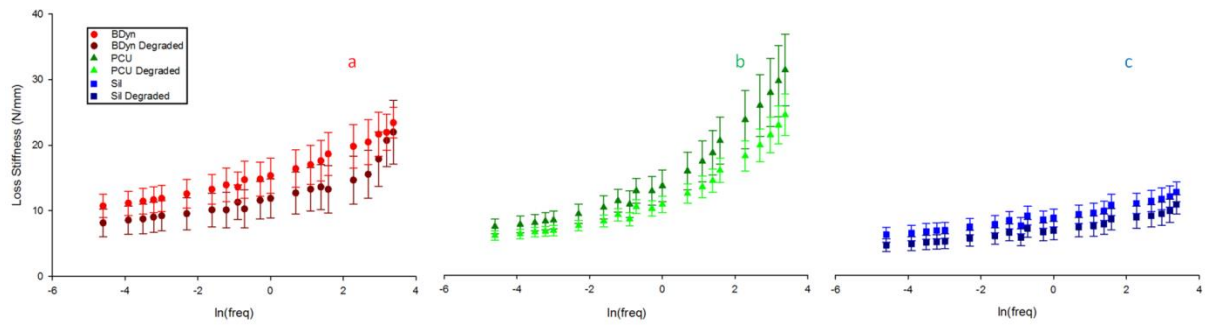
474



475

476 Figure 8: Storage stiffness (k') against $\ln(f)$ for (a) normal and degraded BDyn device (BDyn),
 477 (b) normal and degraded polycarbonate urethane (PCU) component (PCU) and (c) normal
 478 and degraded silicone (Sil) component (mean \pm 95% confidence intervals). Normal data is
 479 from a previous study ⁽⁹⁾.

480



481

482 Figure 9: Loss stiffness (k'') against $\ln(f)$ for (a) normal and degraded BDyn device (BDyn), (b)
 483 normal and degraded polycarbonate urethane (PCU) component (PCU) and (c) normal and
 484 degraded silicone (Sil) component (mean \pm 95% confidence intervals). Normal data is from a
 485 previous study ⁽⁹⁾.

486

487

488 **Table 1: Storage stiffness (equation 4) and loss stiffness (equation 5) regression analyses of the BDyn devices**
489 **and its components. Coefficients (A, B, C and D) for the individual specimens' storage and loss stiffness**
490 **(N/mm) trends are provided.**

Specimen ID	$k' = A \ln(f) + B$				$k'' = C \ln(f) + D$			
	A	B	r ²	P Value	C	D	r ²	P Value
BDyn 1 – 1	2.7	105.1	0.93	<0.001	1.7	16.4	0.90	<0.001
BDyn 1 – 2	1.3	87.0	0.81	<0.001	1.2	11.1	0.80	<0.001
BDyn 1 – 3	1.2	89.6	0.96	<0.001	1.4	14.6	0.81	<0.001
BDyn 1 – 4	0.8	85.1	0.64	<0.001	1.2	11.0	0.82	<0.001
BDyn 1 – 5	3.1	99.4	0.87	<0.001	1.8	15.2	0.80	<0.001
BDyn 1 – 6	1.3	80.3	0.97	<0.001	1.1	8.9	0.77	<0.001
BDyn 1 - Mean	1.7	91.1	0.97	<0.001	1.4	12.9	0.82	<0.001
PCU – 1	6.3	102.7	0.94	<0.001	2.7	14.3	0.90	<0.001
PCU – 2	6.8	123.0	0.96	<0.001	2.5	14.6	0.89	<0.001
PCU – 3	6.3	118.8	0.96	<0.001	2.3	13.7	0.89	<0.001
PCU – 4	5.2	101.2	0.96	<0.001	1.9	11.3	0.88	<0.001
PCU – 5	5.8	107.5	0.95	<0.001	2.1	12.9	0.89	<0.001
PCU – 6	5.1	101.5	0.96	<0.001	1.9	11.3	0.89	<0.001
PCU – Mean	5.9	109.1	0.95	<0.001	2.2	13.0	0.89	<0.001
Silicone – 1	1.1	52.5	0.96	<0.001	0.6	6.2	0.93	<0.001
Silicone – 2	1.5	63.7	0.97	<0.001	0.9	9.5	0.96	<0.001
Silicone – 3	0.7	45.3	0.90	<0.001	0.6	6.0	0.90	<0.001
Silicone – 4	1.4	62.2	0.97	<0.001	0.7	7.6	0.95	<0.001
Silicone – 5	1.1	53.4	0.96	<0.001	0.7	6.5	0.93	<0.001
Silicone – 6	1.2	59.4	0.96	<0.001	0.7	7.8	0.95	<0.001
Silicone - Mean	1.2	56.1	0.97	<0.001	0.7	7.3	0.94	<0.001

491

492

493 **Table 2: Wilcoxon Signed Rank test results for the PCU and Silicone components and Wilcoxon Rank Sum test**
 494 **for the BDyn Device. The frequencies stated indicates a significantly different ($p < 0.05$) between the**
 495 **untreated and degraded specimens.**

Component	Storage Stiffness	Loss Stiffness
PCU	-	0.5 Hz, 4 Hz to 30 Hz
Silicone	0.01 Hz to 30 Hz	0.01 Hz to 30 Hz
BDyn Device	0.2 Hz to 20 Hz	0.01 Hz to 0.3 Hz, 0.5 Hz to 15 Hz

496

497

498

499